doi.org/10.26434/chemrxiv.5659576.v1

Reversible Silver Electrodeposition from Boron Cluster Ionic Liquid (BCIL) Electrolytes

Alexander Spokoyny, Rafal M. Dziedzic, Mary A. Waddington, Sarah E. Lee, Jack Kleinsasser, John B. Plumley, William C. Ewing, Beth D. Bosley, Vincent Lavallo, Thomas L. Peng

Submitted date: 01/12/2017 • Posted date: 05/12/2017

Citation information: Spokoyny, Alexander; Dziedzic, Rafal M.; Waddington, Mary A.; Lee, Sarah E.; Kleinsasser, Jack; Plumley, John B.; et al. (2017): Reversible Silver Electrodeposition from Boron Cluster Ionic Liquid (BCIL) Electrolytes. ChemRxiv. Preprint.

Electrochemical systems offer a versatile means for creating adaptive devices. However, the utility of electrochemical deposition is inherently limited by the properties of the electrolyte. The development of ionic liquids enables electrodeposition in high-vacuum environments and presents opportunities for creating electrochemically adaptive and regenerative spacecraft components. In this work we developed a silver-rich, boron cluster ionic liquid (BCIL) for reversible electrodeposition of silver films. This air and moisture stable electrolyte was used to deposit metallic films in an electrochemical cell to tune the emissivity of the cell in situ, demonstrating a proof-of-concept design for spacecraft thermal control.

Reversible Silver Electrodeposition from Boron Cluster Ionic Liquid (BCIL) Electrolytes

Rafal M. Dziedzic,[†,#] Mary A. Waddington,[†,#] Sarah E. Lee,[‡] Jack Kleinsasser,[‡] John B. Plumley,[§,⊥] William C. Ewing,[I] Beth D. Bosley,[□,*] Vincent Lavallo,[‡,*] Thomas L. Peng,[§,*] Alexander M. Spokoyny.[†,▽,*]

[†]Department of Chemistry and Biochemistry, University of California, Los Angeles, 607 Charles E. Young Drive East, Los Angeles, CA 90095, United States

[‡]Department of Chemistry and Biochemistry, University of California, Riverside, 501 Big Springs Rd., Riverside, CA 92521, United States

[§]Air Force Research Laboratory, Kirtland AFB, New Mexico, United States, Albuquerque, NM 87123, United States

[⊥]Department of Chemistry and Chemical Biology, University of New Mexico, 300 Terrace St. NE, Albuquerque, NM 87131, United States

[I]Boron Specialties LLC, 2301 Duss Avenue, Building 9, Ambridge, PA 15003, United States

[▽]California NanoSystems Institute (CNSI), University of California, Los Angeles, 570 Westwood Plaza, Los Angeles, CA 90095, United States

Supporting Information Placeholder

ABSTRACT: Electrochemical systems offer a versatile means for creating adaptive devices. However, the utility of electrochemical deposition is inherently limited by the properties of the electrolyte. The development of ionic liquids enables electrodeposition in high-vacuum environments and presents opportunities for creating electrochemically adaptive and regenerative spacecraft components. In this work we developed a silver-rich, boron cluster ionic liquid (BCIL) for reversible electrodeposition of silver films. This air and moisture stable electrolyte was used to deposit metallic films in an electrochemical cell to tune the emissivity of the cell *in situ*, demonstrating a proof-of-concept design for spacecraft thermal control.

Keywords: Reversible electrodeposition, ionic liquids, infrared transparent electrochemical cell, boron clusters

Electrodeposited metallic structures are ubiquitous in modern technologies (e. g. batteries, protective coatings, displays, and microchips) and emerging technologies such as resistive memory and reconfigurable electronics.[1,2,3] The broad utility of electrochemically deposited structures grows as new electrolytes enable electrodeposition in increasingly challenging environments. Controlled reversible electrodeposition of metallic structures offers tunable optical properties and electrical conductivity along with the ability to adapt the electrochemical system to changing application needs. This adaptablity is appealling in the context of reconfigurable electronic components which could extend a device's lifetime through *in situ* restructuring.

Early electrodeposition methods used aqueous electrolytes due to the solubility of common metal ions.[1] The development of non-aqueous electrolytes has enabled safe electrodeposition of water sensitive metals for new electrochemical applications such as high density energy storage.[4] Additionally, electrodepostion from

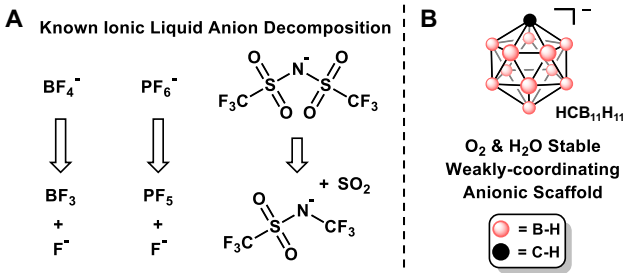

Figure 1. Left, some decomposition products of commonly used ionic liquid anions. Right, monocarborane anion used in this work.

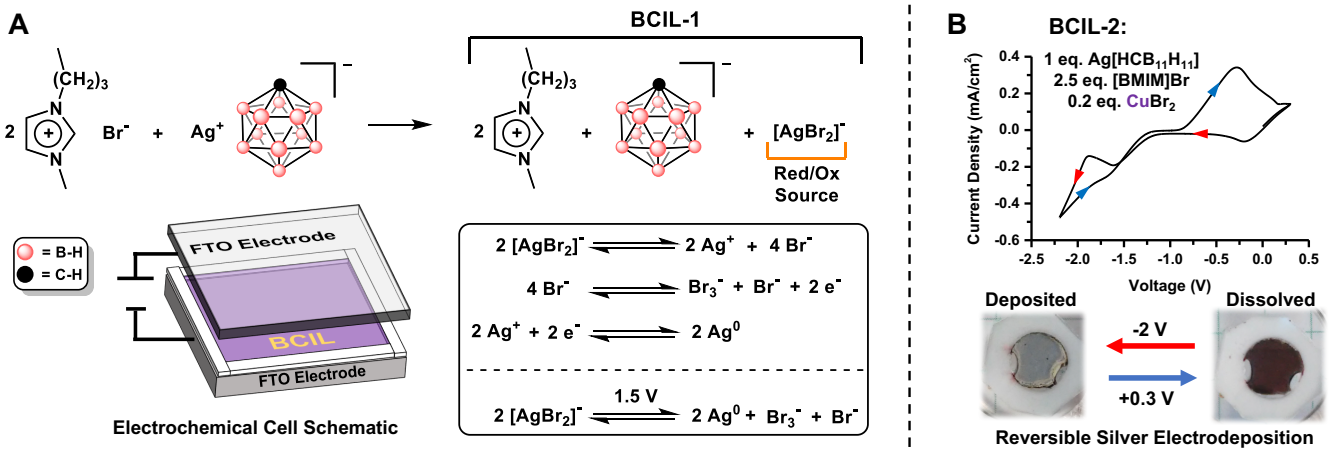

Figure 2. Formation of **BCIL-1** by mixing [BMIM]Br with Ag[$HCB_{11}H_{11}$]. Inset shows the elementary steps associated with silver electrodeposition in **BCIL-1**. Representative cyclic voltamogram of **BCIL-2**, Red and blue arrows indicate cathodic (deposition) and anodic (dissolution) sweep direction respectively.

ionic liquids has emerged as a potential alternative to organic solvent electrolytes and presented new opportunities for electrodeposition in high vacuum and hostile environments such as electron microscopes and plasma chambers.[5,6]

Ionic liquids (ILs), salts with low melting points (typically <100 ºC), combine the high ion solubility of aqueous media, the chemical flexibility of organic solvents, and low volatility and wide electrochemical windows achievable with molten salts.[7] The versatility of ILs is increased by tailoring the cation-anion pairs for individual applications.[7] Yet, despite the numerous cation-anion pairs that can form ionic liquids, much of ionic liquid tunability is achieved by modifying the cationic component.[7] This disparity is largely due to the synthetic availability of cationic molecular scaffolds such as ammonium, phosphonium, and heterocyclic motifs. Conversely, ionic liquids in which the anionic component engenders the IL properties are scarce and the anions are seldom amenable to additional functionalization.[8] Furthermore, the relative instability of commonly used IL anions limits the longevity of IL-based electrochemical devices. This becomes especially problematic when designing systems which require prolonged operation time. Therefore we sought to develop an ionic liquid that contains a highly stable and easily tunable anionic core. Such "anion-based" ILs could use the metal of interest as the cation and enable high metal loadings suitable for rapid electrodeposition. Anionic polyhedral boranes represent a class of modular molecular building blocks suitable for designing "anion-based" **b**oron **c**luster **i**onic **l**iquids (BCILs). Their robust boron-cluster framework provides an anionic scaffold amenable to tuning of melting point, solubility, and redox potential.[9,10] In this work, we set out to develop an all-ionic electrolyte suitable for reversible deposition of silver films. Specifically, we describe an all-ionic electrolyte to reversibly deposit silver films for the purpose of controlling infrared (IR) emission from an electrochemical cell. This technology complements exisiting approaches to controling thermal emission from spacecraft surfaces.[11,12] Importantly, BCILs represent a critical component allowing these devices to perform reliably without having to exclude air and moisture; common contaminants that are introduced during electrochemical device assembly that are difficult to remove.

Silver films play an important technological role as electrical conductors and optical coatings. Silver offers unique advantages over other transition metals because of its high spectral reflectivity, high electrical conductivity and corrosion resistance.[13] These qualities make silver an attractive metal for tuning the properties of spacecraft surfaces. Additionally, the low volatility of IL electrolytes offers a means of performing electrodeposition in high vacuum environments. Due to its positive reduction potential, only small volatages are required to electrodeposit silver from ionic salt precursors.[1] Electrodeposition of silver was historcially performed using cyanide-based electrolytes due to the formation of stable $Ag(CN)_x^{1-x}$ complexes.[1] However the toxicity of aqueous cyanide baths lead to the development of silver electrodeposition from ILs and organic solvents.[4,5] These non-aqueous electrolytes were suitable for reversible silver electrodeposition and served as proof-of-concept works for electrochemically modulated optical films.[8f,15] The reversibility in these systems is attained from the halide-trihalide redox couples (X^-/X_3^-, X = Cl, Br, or I),[16] and stable $[AgX_2]^-$ complexes.[17] Despite these advances, reversibility in all-ionic electrolytes was limited only to a handful of ILs. The majority of these, however, still generate unstable, volatile, or corrosive decomposition products (Figure 1A).[18] In this report, we detail our work on creating an electrolyte for silver deposition containing a stable anion amenable to additional functionalization.

We developed a salt metathesis reaction between 1-butyl-3-methyl-imidazolium bromide, [BMIM]Br, and silver monocarborane, Ag[$HCB_{11}H_{11}$], to generate a boron cluster ionic liquid, **BCIL-1,** with high silver content (Figure 2A). The parent carborane salt can be easily synthesized via a salt metathesis reaction between Cs[$HCB_{11}H_{11}$] and $AgNO_3$ with an 82% yield.[19] This ionic liquid, features an inert ionic matrix of $[BMIM]^+$ and $[HCB_{11}H_{11}]^-$ ions with $[AgBr_2]^-$ ions acting as the primary redox species (Figure 2A). Dialkylimidazolium cations and monocarborane anions were selected due to their electrochemical stability and weakly-coordinating characteristics suitable for designing an inert ionic matrix.[20] The BCILs were enclosed between two FTO electrodes to form transparent, two-electrode electrodeposition cell (Figure 2A). One FTO electrode was set as the working electrode while the other was set as both the counter and reference electrode. Cyclic voltamograms (CVs) show a reduction peak corresponding to reduction of silver complexes to form silver deposits at the working electrode (Figure 2 and 3). Electrodeposition begins at -1.5 V *vs*. FTO with a distinct current loop occurring in the cathodic region, which indicates a nucleation-limited deposition. Reversing the polarity of the electrochemical cell toward +0.3 V *vs*. FTO leads to dissolution of the silver deposits at the working electrode back into the electrolyte. It was also observed that halide and metal ion addives can affect the rate of the silver deposition and etching (Figure 2B

and Figure 3). A general feature of these IL based electrolytes is an excess of halide, X^- (X = Br or Cl) to Ag^+. Typically, X^-:Ag^+ ion ratios of 2.5:1 were sufficient to fully dissolve the silver salts at room temperature. The excess halide promotes the formation of $AgBr_x^{1-x}$ species and provides additional halide ions to access the halide-trihalide (X^-/X_3^-) redox couple.

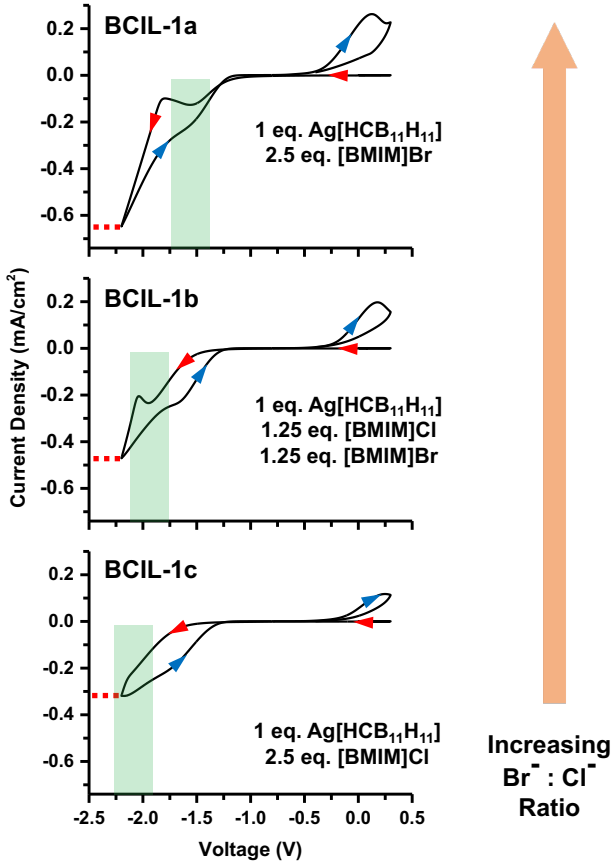

Figure 3. Two-electrode cyclic voltamograms of **BCIL-1** without $CuBr_2$ additive. Increasing the Br^-:Cl^- ratio increases the electrodeposition current. Red and blue arrows indicate cathodic and anodic sweep direction respectively. Green areas indicate the composition dependent FTO | $[AgX_2]^-$, X_3^- | Ag^0 | FTO process, red dashed lines indicate the maximum electrodeposition current density at -2.3 V *vs*. FTO.

As the composition of the electrolyte, with a fixed halide concentration, is varied from chloride-rich to bromide-rich the potential for silver electrodeposition shifts to less cathodic potentials (Figure 3). This dependence on halide identity in the BCIL provides a simple method for tuning the voltage onset and current magnitude of silver electrodeposition. Similar irreversible behavior in previously reported optical modulation devices were resolved by adding Cu(II) salts.[15] Related studies on the effects of $CuBr_2$ in [BMIM]Br ionic liquids found that $CuBr_2$ complexes were as effective at etching copper films as H_2SO_4.[21] Likewise, addition of 10 mol % $CuBr_2$ (relative to Ag^+) to **BCIL-1** dramatically improved the reversibility of the ionic liquid formulation, generating **BCIL-2** (Figure 2B). Noteworthy was the change in film dissolution dynamics, wherein silver films deposited in the presence of Cu(II) were readily removed and exhibited larger oxidative currents (Figure 2B and SI).[22]

Previously, it has been shown that water content present in ILs during their ambient handling can alter the reversibility of silver deposition.[23] Importantly, **BCIL-2** containing devices placed into a 98% humidity chamber did not experience alterations in device performance. CV experiments showed identical operating currents even after 4 days at these conditions. Such water tolerance enabled an easy benchtop assembly. Despite the electrochemical and moisture stability of **BCIL-2**, a gradual decrease in electrodeposition current was observed during electrochemical cycling of **BCIL-2** cells (see SI). After leaving the electrochemical cell overnight at room temperature, the electrodeposition current through the cell decayed and redox features became indistinguishable (Figure 4A). Visual inspection of the electrolyte showed formation of visible microcrystallites. Heating the cell to 60°C for 1 hour dissolved the visble crystallites thereby restoring the cell to the original performance. This ultimately suggests that formation of small crystallites leads to reduced ion mobility and electrodeposition current.

Contrary to prevailing approaches of changing the physical properties of ILs by altering the cation, we sought to inhibit crystallite formation by functionalizing the monocarborane anion. A third electrolytic mixture, **BCIL-3**, was prepared using a monocarborane functionalized with a *sec*-butyl group appended on the carbon vertex of the boron-rich cluster (Figure 4B). After the electrochemical cell containing **BCIL-3** was kept at room temperature for 24 hours the deposition currrents were comparable to those obtained from freshly prepared **BCIL-3** suggesting that, at this timescale, no obeservable crystallization occurs and hence the device performance remains unaffected. Heating of the **BCIL-3** cell to 60°C for 1 hour further increased the electrodeposition current and eliminated the hysteresis current loop completely (see SI).

The quality of the electrodeposited films was monitored using a 633 nm laser to correlate the film growth to the electrochemical behavior of the cells. Extended electrochemical cycling of a **BCIL-3** cell revealed a decay in reflectance change (Figure 4C), likely due to partial crystallization of **BCIL-3**. These effects were mitigated by heating the cell every 40 cycles (Figure 4C) to restore reflectance changes of up to 80%.

The silver film electrodeposition from **BCIL-3** can reach maximum reflectance within ~ 3 seconds when applying a -2.5 V cathodic potential, and it can be quickly removed by reversing the polarity of the electrochemical cell to +2.5 V (Figure 4C). Oxidative etching of the electrodeposited silver film is likely accelerated by electromigration of halides toward the working electrode and subsequent removal of electrodeposited silver as solvated silver halide anions.[15] Applying a voltage (-1.8 V) for 450 seconds produced a thick film, which could be analyzed by scanning electron microscopy (SEM).[24] Consistent with nucleation-limited deposition, the silver deposits grow as a film of silver crystallites approximately 500 nm in diameter (Figure 5). EDX elemental mapping shows two types of silver-containing deposits; an underlying Ag film with AgBr crystals on top of the film.The AgBr deposits likely formed during the washing of the working electrode, as described previously.[15b]

Having identified a suitably resilient electrolyte capable of depositing silver films, we set out to control the IR emission

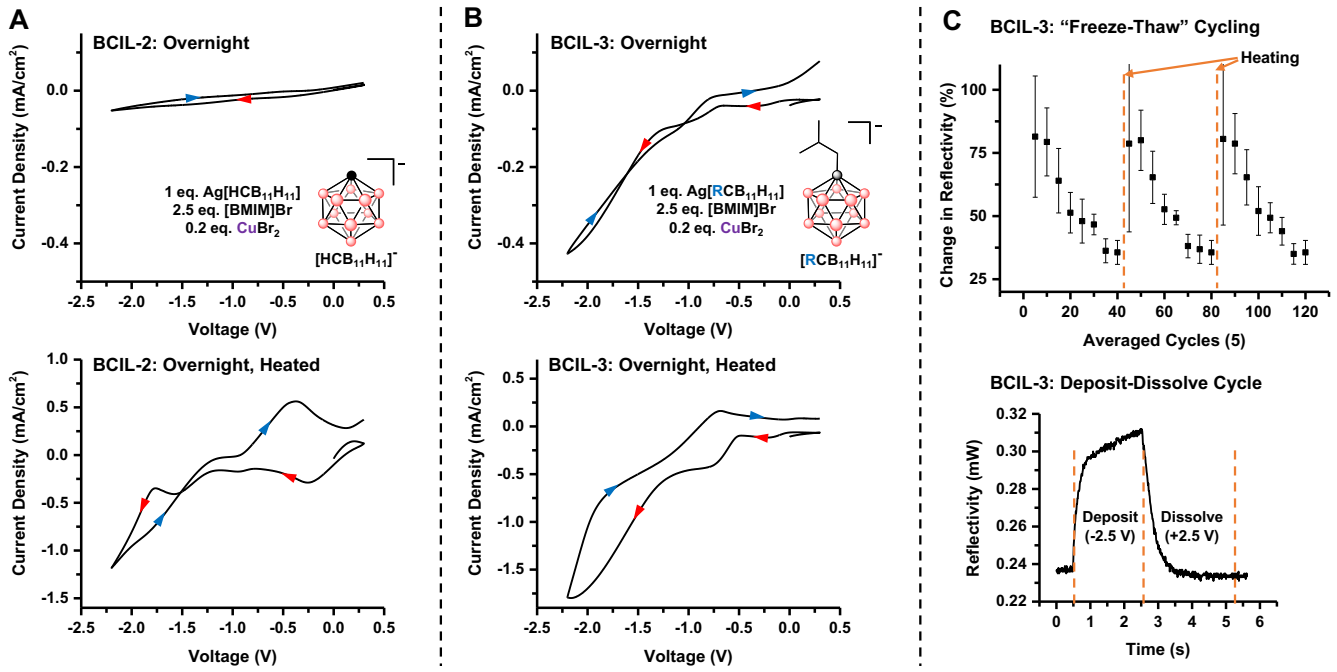

Figure 4. A) Two-electrode cyclic voltamograms of **BCIL-2** after equilibrating at ambient conditions overnight and after heating the equilibrated cell to 60 °C, top and bottom respectively. B) Two-electrode cyclic voltamograms of **BCIL-3** after equilibrating at ambient conditions overnight and after heating the equilibrated cell to 60 °C, top and bottom respectively. Red and blue arrows indicate cathodic and anodic sweep direction respectively. C) Change in reflectivity (Δρ) at 633 nm of **BCIL-3** electrochemical cell during extended "freeze-thaw" cycling and during a single deposition-dissolution cycle, top and bottom respectively. The electrochemical cell was regenerated every 40 cycles by heating to 60 °C.

of the electrochemical cell by depositing a metallic film. From the law of conservation of energy, the sum of the absorption/emission (α/ε), transmission (τ), and reflection (ρ) interactions of an incident electromagnetic wave must sum to unity (Eq. 1).[25]

$$\alpha + \rho + \tau = 1 = \varepsilon + \rho + \tau \text{ (Eq. 1)}$$
$$\alpha = \varepsilon$$

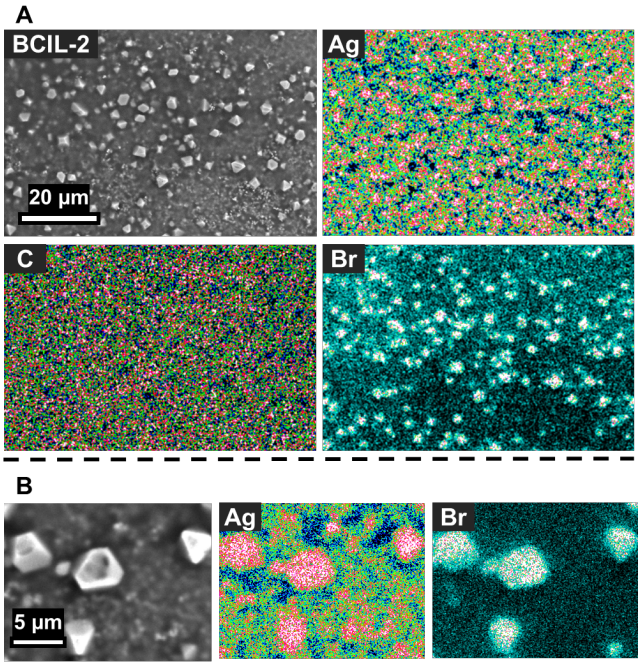

Figure 5. A) Scanning electron micrographs and EDX elemental mapping of **BCIL-3** working electrode after deposition of a silver film. B) Magnified scanning electron micrographs and EDX elemental mapping showing a silver film beneath AgBr deposits.

As such, a perfect blackbody radiator (α = ε = 1) is not reflective (ρ = 0) because the absorption term dominates Eq. 1. Conversely, a perfectly reflective surface (ρ = 1) would not absorb/emit energy (α = ε = 0). Thus, the emissivity (ε) of a fixed transparency object can be altered by changing the surface reflectivity (ρ) (Eq. 2).

$$\Delta \varepsilon = -\Delta\rho \text{ (Eq. 2)}$$

Similarly, electrodeposition of a reflective film onto an IR emitter would block the IR emission of the underlying IR sources (e.g. electrolyte and counter electrode), see SI for demonstration.[11,12,26] Such variable emissivity materials serve as the basis for adaptive surfaces for spacecraft thermal control. However, environmental instability and slow switching times limit their wide-spread application.

Metal-rich, all-ionic electrolytes can offer the vacuum stability of solid-state materials and rapid deposition rates of liquid electrolytes. A proof-of-concept IR transparent electrochemical cell was fabricated by enclosing **BCIL-3** between two IR transparent conductors composed of a 200 nm ITO film deposited onto a sapphire (Al_2O_3) window which is IR transmission up to ~6 μm. The electrochemical cell was mounted in an FTIR spectrometer with the working electrode facing the detector and IR transmission spectra were collected for the REM in the unplated and plated states (Figure 5). Electrodeposition of a metallic film reduced the IR transmission by ~18% across the measurement window, indicating that the deposition of a reflective film blocked the emission of the underlying IR sources. Strong absorption at ~3000 and ~2400 cm^{-1} is attributed to the imidazolium and carborane ions respectively. Although the longevity of the IR transparent cell was limited by the ITO electrode instability (see SI), it showcases the potential liquid-based technologies achieveable with ionic liquids.

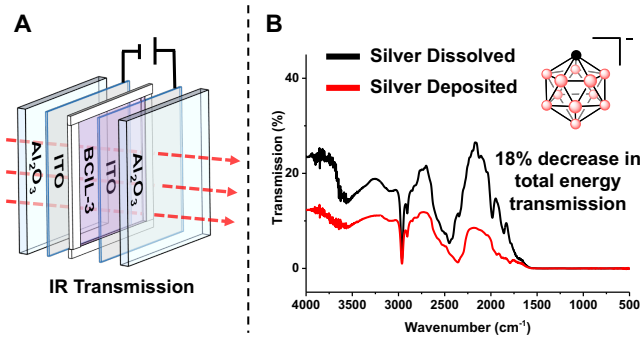

Figure 6. A) schematic of IR transparent electrochemical cell. B) FTIR transmission spectrum of **BCIL-3** IR transparent cell before and after silver film electrodeposition.

In summary, we prepared a stable, all-ionic electrolyte designed around the weakly coordinating carborane framework for reversible electrodeposition of silver films. The metal-rich electrolyte enables rapid, reversible silver electrodeposition. Meanwhile, the ionic composition presents opportunities for electrodeposition in extreme environments (such as high temperature and low pressure). We demonstrate the utility of this electrolyte in electrochemically modulated optical devices.

ASSOCIATED CONTENT

Supporting Information

Full procedures and crystallographic and other characterizing data are provided in the supporting information, which is available free of charge at **http://pubs.acs.org**.

AUTHOR INFORMATION

Corresponding Authors

beth@boron.com (B.D.B.)
vincent.lavallo@ucr.edu (V.L.)
thomas.peng.3@us.af.mil (T.L.P.)
spokoyny@chem.ucla.edu (A.M.S.)

Author Contributions

#These authors contributed equally to the work.

Notes

The authors declare no competing financial interests.

ACKNOWLEDGMENTS

Authors thank the Air Force Research Laboratory for funding through STTR program (Topic AF16-AT20). A.M.S. acknowledges the Department of Chemistry and Biochemistry at UCLA for start-up funds and the NSF for partial support (CHE-1048804). A.M.S. also thanks 3M for a Non-Tenured Faculty Award and Alfred P Sloan Foundation for the Sloan Research Fellowship support. R.M.D. thanks the National Defense Science and Engineering Graduate Fellowship Program for support.

REFERENCES

(1) Modern Electroplating, Schlesinger, M and Paunovic, M. 2014, John Wiley & Sons, Inc. Hoboken 2014.

(2) a) Deligianni, H.; Ahmed, S.; Romankiw, L. *Electrochem. Soc. Interface* **2011**, *20*, 47-53. b) Armand, M.; Endres, F.; MacFarlane, D. R.; Ohno, H.; Scrosati, B. *Nat. Mater.* **2009**, *8*, 621-629.

(3) a) Kim, M.-K.; Lee, J.-S. *ACS Appl. Mater. Interfaces* **2016**, *8*, 32918-32924. b) Harada, A.; Yamaoka, H.; Watanabe, K.; Kinoshita, K.; Kishida, S.; Fukaya, Y.; Nokami, T.; Itoh, T. *Chem. Lett.* **2015**, *44*, 1578-1580. c) Wang, Z.; Joshi, S.; Savel'ev, S. E.; Jiang, H.; Midya, R.; Liu, P.; Hu, M.; Ge, N.; Strachan, J. P.; Li, Z.; Wu, Q.; Barnell, M.; Li, G.-L.; Xin, H. L.; Williams, R. S.; Xia, Q.; Yang, J. J. *Nat. Mater.* **2017**, *16*, 101-108. d) Jo, S. H.; Chang, T.; Ebong, I.; Bhadviya, B. B.; Mazumder, P.; Lu, W. *Nano Lett.* **2010**, *10*, 1297-1301. e) Waser, R.; Aono, M. *Nat. Mater.* 2007, *6*, 833-840.

(4) Simka, W.; Puszczyk, D.; Nawrat, G. *Electrochim. Acta* **2009**, *54*, 5307-5319.

(5) a) Zhang, Q.; Wang, Q.; Lu, X.; Zhang, X. *ChemPhysChem* **2016**, *17*, 335-351. b) Liu, F.; Deng, Y.; Han, X.; Hu, W.; Zhong, C. *J. Alloys Compd.* **2016**, *654*, 163-170. c) Watanabe, M.; Thomas, M. L.; Zhang, S.; Ueno, K.; Yasuda, T.; Dokko, K. *Chem. Rev.* **2017**, *117*, 7190-7239.

(6) Kuwabata, S.; Tsuda, T.; Torimoto, T. *J. Phys. Chem. Lett.* **2010**, *1*, 3177-3188.

(7) Abbott, A. P.; McKenzie, K. J. *Phys. Chem. Chem. Phys.* **2006**, *8*, 4265-4279.

(8) a) Zeng, Z.; Twamley, B.; Shreeve, J. *Organmetallics* **2007**, *26*, 1782-1787. b) Hog, M.; Schneider, M.; Krossing, I. *Chem. Eur. J.* **2017**, 23, 9821-9830. c) Türp, D.; Wagner, M.; Enkelmann, V.; Müllen, K. *Angew. Chem. Int. Ed.* **2011**, *50*, 4962-4965. d) Shkrob, I. A.; Marin, T. W.; Wishart, J. F. *J. Phys. Chem. B* **2013**, *117*, 7084-7094. e) Xie, H. J.; Gélinas, B.; Rochefort, D. *Electrochim. Acta* **2016**, *200*, 283-289. f) Deng, M.-J.; Chen, P.-Y.; Leong, T.-l.; Sun, I-W.; Chang, J.-K.; Tsai, W.-T. *Electrochem. Commun.* **2008**, *10*, 213-216. f) Gelinas, B.; Das, D,; Rochefort, D. *ACS Appl. Mater. Interfaces* **2017**, *9*, 28726-28736.

(9) a) Zhu, Y.; Hosmane, N. S. *Eur. J. Inorg. Chem.* 0000, 0, 0 [DOI: 10.1002/ejic.201700553]. b) Sivaev, I. B. *Chem. Het. Comp.* **2017**, *53*, 638-658. c) Liu, S.; Chen, Z.; Zhang, Q.; Zhang, S.; Li, Z.; Shi, F.; Ma, X.; Deng, Y. *Eur. J. Inorg. Chem.* **2011**, 1910-1920. d) Dymon, J.; Wibby, R.; Kleingardner, J.; Tanski, J. M.; Guzei, I. A.; Holbrey, J. D.; Larsen, A. S. *Dalton Trans.* **2008**, *0*, 2999-3006. e) Larsen, A. S.; Holbrey, J. D.; Tham, F. S.; Reed, C. A. *J. Am. Chem. Soc.* **2000**, *122*, 7264-7272. f) Matsumi, N.; Miyamoto, M.; Aoi, K. *J. Organomet. Chem.* **2009**, *694*, 1612-1616. g) Rak, J.; Jakubek, M.; Kaplánek, R.; Král, V. *Inorg. Chem.* **2012**, *51*, 4099-4107. h) Nieuwenhuyzen, M.; Seddon, K. R.; Teixidor, F.; Puga, A. V.; Viñas, C. *Inorg. Chem.* **2009**, *48*, 889-901. i) Wixtrom, A. I.; Shao, Y.; Jung, D.; Machan, C. W.; Kevork, S. N.; Qian, E. A.; Axtell, J. C.; Khan, S. I.; Kubiak, C. P.; Spokoyny, A. M. *Inorg. Chem. Front.* **2016**, 3, 711-717. j) Messina, M. S.; Axtell, J. C.; Wang, Y.; Chong, P.; Wixtrom, A. I.; Kirlikovali, K. O.; Upton, B. M.; Shafaat, O. S.; Khan, S. I.; Winkler, J. R.; Gray, H. B.; Alexandrova, A. N.; Maynard, H. D.; Spokoyny, A. M. *J. Am. Chem. Soc.* **2016**, *138*, 6952-6955.

(10) a) Justus, E.; Rischka, K.; Wishart, J. F.; Werner, K.; Gabel, D. *Chem. Eur. J.* **2008**, *14*, 1918-1923. b) Bertocco, P.; Derendorf, J.; Jenne, C.; Kirsch, C. *Inorg. Chem.* **2017**, *56*, 3459-3466. c) McArthur, S. G.; Jay, R.; Geng, L.; Guo, J.; Lavallo, V. *Chem. Commun.* **2017**, *53*, 4453-4456.

(11) a) Demiryont, H.; Shannon III, K. *AIP Conf. Proc.* 2007, *880*, 51. b) Shannon III, K. C.; Sheets, J.; Groger, H.; Williams, A. *Proc. of SPIE* **2009**, *7330*, 73300F. c) Mason, J. A.; Smith, S.; Wasserman, D. *Appl. Phys. Lett.* **2011**, *98*, 241105. d) Chandrasekhar, P.; Zay, B. J.; Lawrence, D.; Caldwell, E.; Sheth, R.; Stephan, R.; Cornwell, J. *J. Appl. Polym. Sci.* **2014**, *131*, 40850. e) Farrar, D.; Douglas, D. M.; Swanson, T.; Collins, C.; Darrin, A.; Osiander, R. *AIP Conf. Proc.* **2007**, *73*, 880. f) Osiander, R.; Firebaugh, S. L.; Champion, J. L.; Farrar, D.; Garrison Darrin, M. A. *IEEE Sensors Journal* **2004**, *4*, 525-

(12) Bergeron, B. V.; White, K. C.; Boehme, J. L.; Gelb, A. H.; Joshi, B. P. *J. Phys. Chem. C* **2008**, *112*, 832-838.

(13)CRC Handbook of Chemistry and Physics, 98th ed.; Rumble, J. R., Ed.; CRC Press/Taylor & Francis: Boca Raton, FL, (Internet Version 2018).

(14) Reyna-González, J. M.; Reyes-López, J. C.; Aguilar-Martínez, M. *Electrochim. Acta* **2013**, *94*, 344-352

(15) a) Camlibel, I.; Singh, S.; Stocker, H. J.; Van Uitert, L. G.; Zydzik, G. *J. Appl. Phys. Lett.* **1978**, *33*, 793-784. b) Van Uitert, L. G.; Camlibel, I.; DeLaRue, R. M.; Kyle, T. R.; Pawelek, R.; Sing, S.; Stocker, H. J.; Zydzik, G. J. *Appl. Phys. Lett.* **1979**, *34*, 232-234. c) Stocker, H. J.; Van Uitert, L. G.; Loomis, T. C.; Koch, F. B. *J. Electrochem. Soc.* **1981**, *128*, 746-748. d) Mascaro, L. H.; Kaibara, E. K.; Bulhões, L. O. *J. Electrochem. Soc.* **1997**, *144*, L273-L274. Lu, W.; Fadeev, A. G.; Qi, B.; Mattes, B. R. *J. Electrochem. Soc.* **2004**, *151*, H33-H39.

(16) a) Popov, A. I.; Geske, D. H. *J. Am. Chem. Soc.* **1958**, *80*, 5346-5349. b) Nelson, I. V.; Iwamto, R. T. *J. Electroanal. Chem.* **1964**, *7*, 218-

221. c) Allen, G. D.; Buzzeo, M. C.; Villagrán, C.; Hardacre, C.; Compton, R. G. *J. Electroanal. Chem.* **2005**, *575*, 311-320. e) Thanthiriwatte, K. S.; Spruell, J. M.; Dixon, D. A.; Christe, K. O.; Jenkins, H. D. B. *Inorg. Chem.* **2014**, *53*, 8136-8146.

(17) Luehrs, D. C.; Iwamoto, R. T.; Kleinberg, J. *Inorg. Chem.* **1966**, *5*, 201-204.

(18) a) Swatloski, R. P.; Holbrey, J. D.; Rogers, R. D. *Green Chem.* **2003**, *5*, 361-363. b) Freire, M. G.; Neves, C. M. S. S.; Marrucho, I. M.; Coutinho, J. A. P.; Fernandes, A. M. *J. Phys. Chem. A* **2010**, *114*, 3744-3749. c) Chambreau, S. D.; Schenk, A. C.; Sheppard, A. J.; Yandek, G. R.; Vaghjiani, G. L.; Maciejewski, J.; Koh, C. J.; Golan, A.; Leone, S. R. *J. Phys. Chem. A* **2014**, *118*, 11119-11132. d) Wang, B.; Qin, L.; Mu, T.; Xue, Z.; Gao, G. *Chem. Rev.* **2017**, *117*, 7113-7131. e) Zaitsau, D. H.; Yermalayeu, A. V.; Emel'yanenko, V. N.; Butler, S.; Schubert, T.; Verevkin, S. P. *J. Phys. Chem. B* **2016**, *120*, 7949-7957. f) Zaitsau, D. H.; Paulechka, Y. U.; Kabo, G. J. *J. Phys. Chem. A* **2006**, *110*, 11602-11604.

(19) a) Shelly, K.; Finster, D. C.; Lee, Y. G.; Scheidt, W. R.; Reed, C. A. *J. Am. Chem. Soc.* **1985**, *107*, 5955. b) Kleinsasser, J. F.; Fisher, S. P.; Tham, F. S.; Lavallo, V. *Eur. J. Inorg. Chem.* **2017**, *38-39*, 4417-4419.

(20) a) Ngo, H. L.; LeCompte, K.; Hargens, L.; McEwen, A. B. *Thermochimica Acta* **2000**, *357-358*, 97-102. b) Douvris, C.; Michl, J. *Chem. Rev.* **2013**, *113*, PR179-PR233.

(21) a) Grishina, E. P.; Pimenova, A. M.; Kuryakova, N. O. *Russ. J. Electrochem.* **2012**, *48*, 1166-1170. b) Grishina, E. P.; Kudryakova, N. O.; Ramenskaya, L. M.; Pimenova, A. M.; Ivanov, V. K. *Surf. Coat. Technol.* **2015**, *272*, 246-253. c) Grishina, E. P.; Kudryakova, N. O.; Pimenova, A. M. *Prot. Met. Phys. Chem. Surf.* **2017**, *53*, 663-669. d) de Oliveira, S. C.; de Morais, L. C.; da Silva Curvelo, A. A.; Torresi, R. M. *J. Electrochem. Soc.* **2003**, *150*, E578-E582.

(22) a) Dali, S.; Benghanem, F.; Khan, M. A.; Meullemeestre, J.; Vierling, F. *Polyhedron* **1991**, *10*, 2529-2533. b) Sestili, L.; Furlani, C.; Ciana, A.; Garbassi, F. *Electrochim. Acta* **1970**, *15*, 225-235.

(23)Basile, A.; Bhatt, A.I.; O'Mullane, A. P.; Bhargava, S. K. *Electrochim. Acta* **2011**, *56*, 2895-2905.

(24) SEM studies required thicker Ag films due to etching of the films by solvent used to remove excess BCIL and expose the underlying Ag deposits. See reference 15c.

(25) G. B. Rybicki, A. P. Lightman, Fundamentals of Radiative Transfer, Radiative Processes in Astrophysics, Wiley-VCH, 2004.

(26) J. F. Clawson, G. T. Tsuyuki, B. J. Anderson, C. G. Justus, W. Batts, D. Ferguson, D. G. Gilmore, Spacecraft Thermal Environments, pg 21-69, Spacecraft Thermal Control Handbook, Volume 1: Fundamental Technologies, 2nd Ed., The Aerospace Press, 2002.

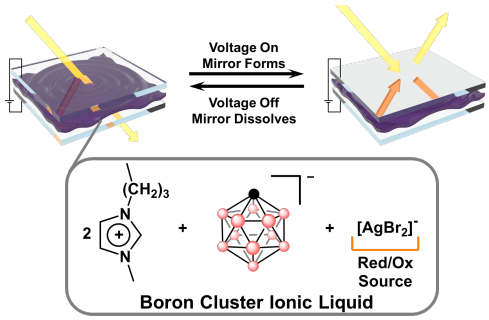

Reversible Silver Electrodeposition from Boron Cluster Ionic Liquid (BCIL) Electrolytes

Rafal M. Dziedzic, Mary A. Waddington, Sara E. Lee, Jack Kleinsasser, John B. Plumley, William C. Ewing, Beth D. Bosley,* Vincent Lavallo,* Thomas L. Peng,* Alexander M. Spokoyny*

SUPPLEMENTARY INFORMATION

Email: spokoyny@chem.ucla.edu, Thomas.peng.3@us.af.mil, vincent.lavallo@ucr.edu, beth@boron.com

Table of Contents

1. General Considerations

Two-electrode symmetrical cells were used to study the electrochemical behavior of the ionic liquid during electrodeposition. The cells were composed of two fluorine-doped tin oxide glass (FTO) separated by a 0.25 mm thick PTFE spacer containing a 9/32" (7.14 mm) diameter hole. The PTFE spacer was coated with a thin layer of silicone grease, placed on the conductive side of the FTO electrode, the PTFE spacer cavity was filled with IL electrolyte, and sealed with a second FTO electrode. All electrochemical cell construction was done in ambient conditions. FTO glass was used instead of tin-doped indium oxide (ITO) because ITO electrodes degraded during electrochemical cycling as judged by the increased resistance of areas exposed to the ionic liquid.

Copper (II) bromide and ($CuBr_2$) were Sigma Aldrich and used without further purification.

Silver monocarborane salt and variants were synthesized as described *infra vide*.

Devices were heated by resting on a hot plate set to 60 °C for 1 hour. Devices were then cooled to room temperature for 1 hour before further testing.

2. Instrumentation

NMR: ^{1}H, ^{11}B, $^{11}B\{^{1}H\}$ NMR spectra were recorded on DRX500, AVIII 500 and AV600 spectrometers in ambient conditions unless stated otherwise. Bruker Topspin V3.2 software was used to process the FID data and MestReNova V10.0.2-15465 software was used to visualize the spectra.

Electrochemistry: Electrochemical analysis was performed using a CH instruments potentiostat.

SEM imaging: Scanning electron micrographs were obtained using a JEOL JSM-IT100 SEM. Energy-dispersive X-ray spectroscopy was obtained using a JEOL electron beam spectrometer.

Thermal Imaging: An FLIR E40 series camera from AZ technology was used for all emissivity imaging.

Reflectivity Measurements: Laser reflectivity measurements were performed using a 633 nm He-Ne laser and Thor Labs S120VC 50mW power meters interfaced with ThorLabs PM100 Multi-Power Meter Software. The experimental configuration consisted of the laser beam striking the center of the electrodeposition cavity from 22.8 cm away and the reflected beam was measured with the power meter 28.0 cm away.

IR Transmission Attenuation: A two-electrode cell was assembled as described above using sapphire substrates coated with a 200 nm thick ITO layer. The cell was mounted in an FT-IR spectrometer and IR transmission spectra were obtained before electrodeposition and after depositing a silver film by applying 2.5 V for 30 seconds. For all cycling measurements, a multi-potential stepping program was used. Specifically, the device was pulsed -1.8 V (15 seconds), 0.6 V (40 seconds), 0.8 V (5 seconds), 0.0 V (30 seconds).

3. Precursor Synthesis

Silver Monocarborane (Ag[$HCB_{11}H_{11}$])

This salt was made according to a literature procedure.[1]

Cesium Monocarborane (Cs[$HCB_{11}H_{11}$])

This salt was made according to a literature procedure.[2]

S-Butyl Siver Monocarborane (Ag[*s*-butyl$CB_{11}H_{12}$])

Li[*closo*-1-$LiCB_{11}H_{11}$] was prepared according to literature[3]: under an inert atmosphere, 5.0 grams of $(CH_3)_3NH$ [$HCB_{11}H_{11}$] was dissolved in 10 mL THF in a 20 mL scintillation vial equipped with a stir bar. 2.2 equivalents of 2.5 M *n*-butyllithium in hexanes was added and the mixture was allowed to stir for 3 hours. The resulting solution was added dropwise to a 250 mL round bottom flask containing 70 mL hexanes while stirring, resulting in a white precipitate. The solvent was decanted and the remaining white precipitate dried under vacuum. The isolated white precipitate was dissolved in 10 mL THF. Two equivalents of 1-iodo-2-methylpropane were added to the reaction solution and stirred for 90 minutes. The solution was removed from inert conditions, organic solvents were removed *in vacuo*, and the crude product was added to 50 mL H_2O. The alkylated carborane product was purified using the following salt exchange procedure: $(CH_3)_3NH$ HCl was added in excess to the aqueous solution, precipitating the $(CH_3)_3NH$ alkyl carborane salt. The solution was filtered and the precipitate was redissolved in approximately 80 mL slightly basic H_2O with an excess of CsCl. The solution was concentrated down to 30-40 mL, and upon cooling to room temperature the Cs^+ salt of the alkylated carborane product precipitated as a white crystalline solid. A concentrated solution of 1.3 grams of Cs^+ 2-methylpropyl-1-carborane, Cs[$(C_4H_9)CB_{11}H_{11}$] was prepared by heating in 50 mL of slightly acidic DI water (3-5 drops of concentrated HNO_3). 1.1 equivalents of $AgNO_3$ was dissolved in 5 mL or less, and added to the aqueous solution. An off-white precipitate formed immediately, and the solution was cooled to room temperature before filtering. Ag[$(C_4H_9)CB_{11}H_{11}$] final yield of 960 mg, 79.7%. ^{1}H NMR (300 MHz, acetone-d_6, 25°C): δ = 2.83 – 0.45 (bm, 11H, B-H), 1.61 (d, 2H, $^3J(H,H)$ = 2.0 Hz) 1.54 (m, 1H), 0.71 (d, 6H, $^3J(H,H)$ = 2.0 Hz) ppm. ^{11}B[^{1}H] NMR (96 MHz, acetone-d_6, 25°C): δ = -8.3, -9.7 ppm. ^{11}B NMR (96 MHz, acetone-d_6, 25°C): δ = -8.2 ppm ($^1J(H,B)$ = 145.0 Hz), -9.7 ppm ($^1J(H,B)$ = 128.6 Hz).

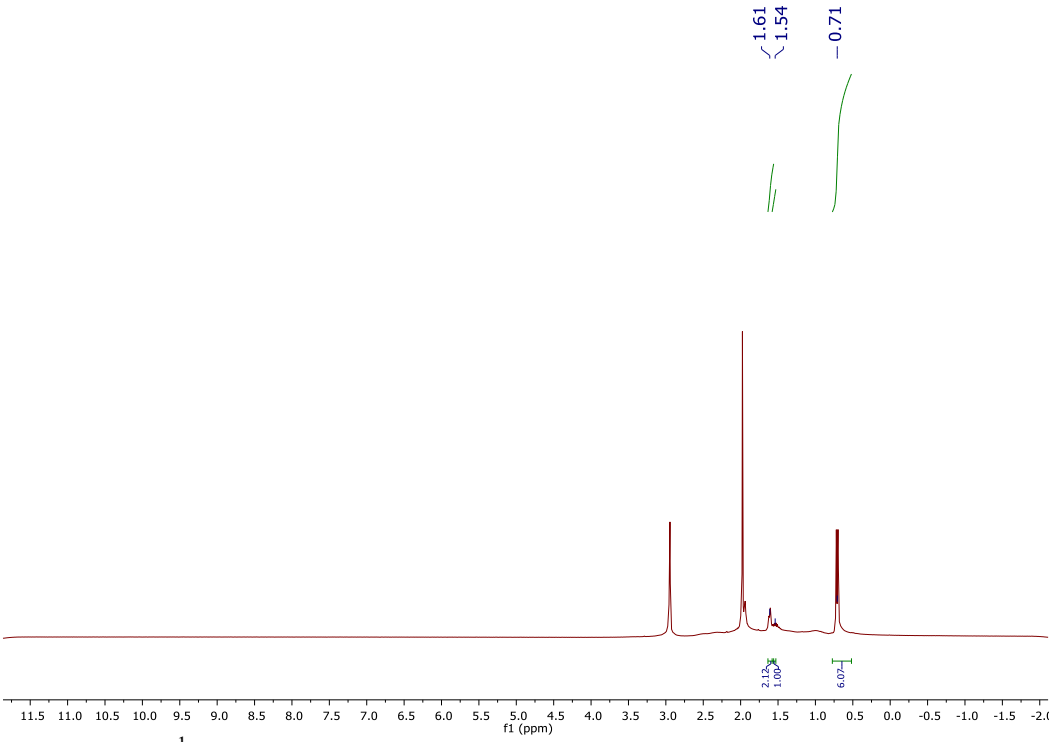

Figure S1A. ^{1}H-NMR spectrum of **Ag[$(C_4H_9)CB_{11}H_{11}$]** in acetone-d_6. *Note: peak at 2.80 ppm is from H_2O .*

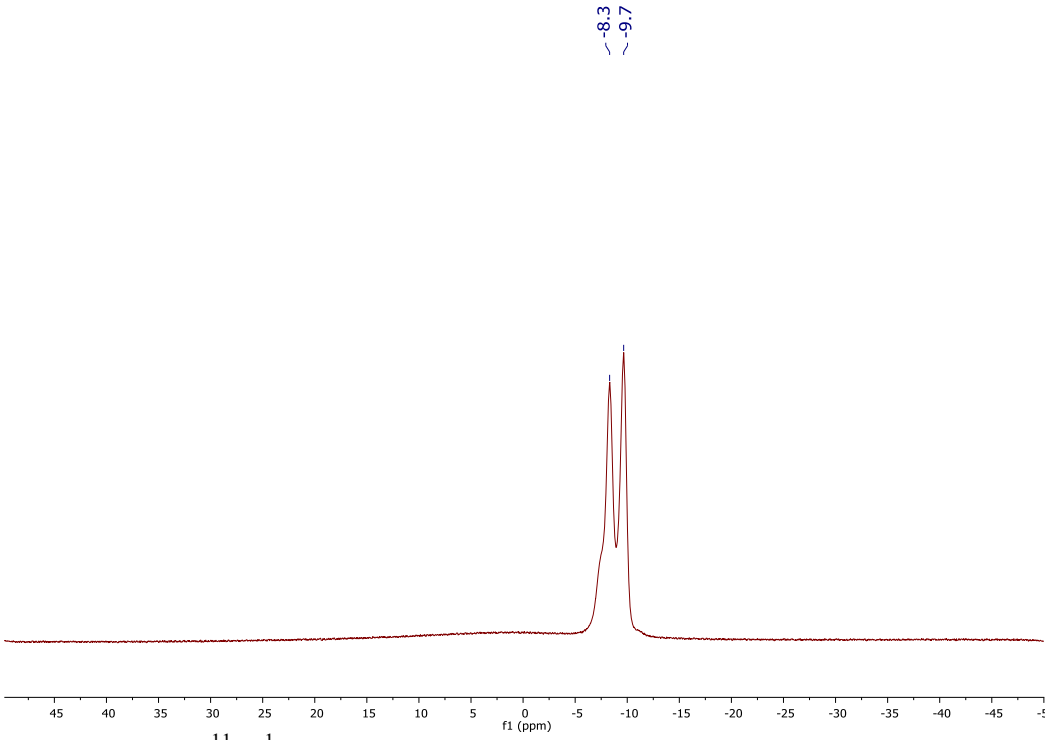

Figure S1B. ^{11}B[^{1}H]-NMR spectrum of **Ag[$(C_4H_9)CB_{11}H_{11}$]** in acetone-d_6.

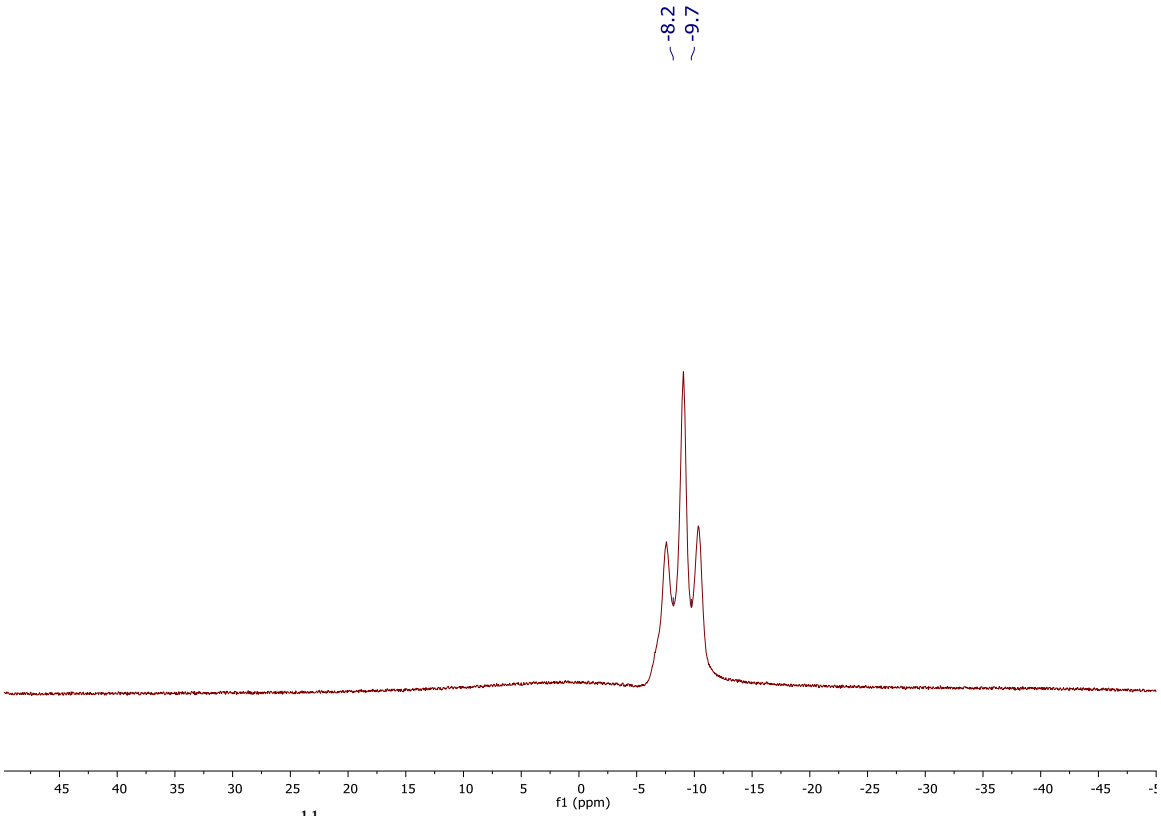

Figure S1C. ^{11}B-NMR spectrum of **Ag[$(C_4H_9)CB_{11}H_{11}$]** in acetone-d_6

4. BCIL Formulation

BCILs were prepared by mixing 1-butyl-3-methyl-imidazolium bromide ([BMIM]Br), silver monocarborane, and $CuBr_2$ in a 4 mL vial with gentle heating to ~50 ºC to facilitate mixing. A molar ratio of 2.5 ([BMIM]Br): 1.0 silver monocarborane: 0.2 $CuBr_2$ was maintained for all BCIL formulations. Once the BCIL became homogeneous, atmospheric moisture was removed under vacuum with mild heating until the BCIL stopped outgassing. Note: extended exposure to atmospheric moisture leads to a teal colored BCIL, likely due to formation of copper aqua complexes. The original performance of the BCIL can be recovered by dehydrating the BCIL with mild heating under vacuum.

5. Normalization of CV Currents

All electrochemical current was normalized to the electrode area, 0.489 cm^2. The same working area was used for all studies.

6. Moisture Stability Studies

The assembled device was placed into an Associated Environmental Systems humidity chamber and set to 98% humidity at room temperature for 4 days. CVs exhibit equivalent currents and redox features even after 4 days of moisture exposure.

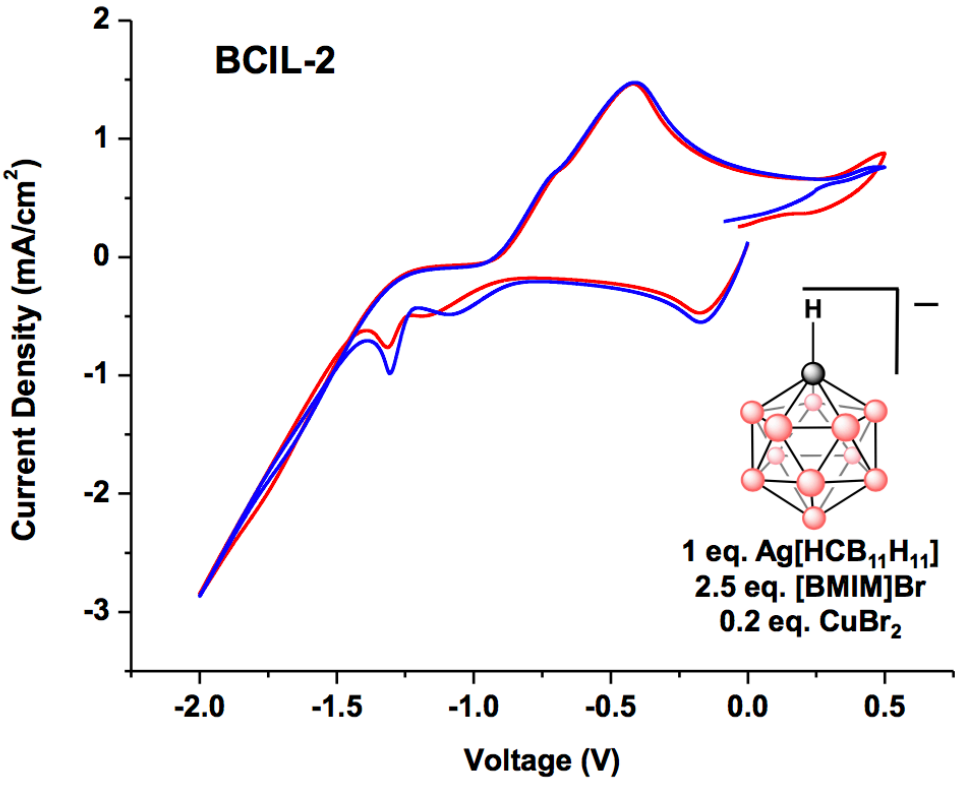

Figure S2. Cyclic voltammograms of BCIL-2 before placement into moisture chamber (blue) and after 4 days of exposure at 98% humidity (red).

7. Electrochemical Current Reductions

BCIL-2 Current Loss

Gradual current decay was observed upon extended cycling of BCIL-2. After 100 cycles, current had dropped to zero This decay is current is attributed to a loss of ion mobility and gradual crystallization.

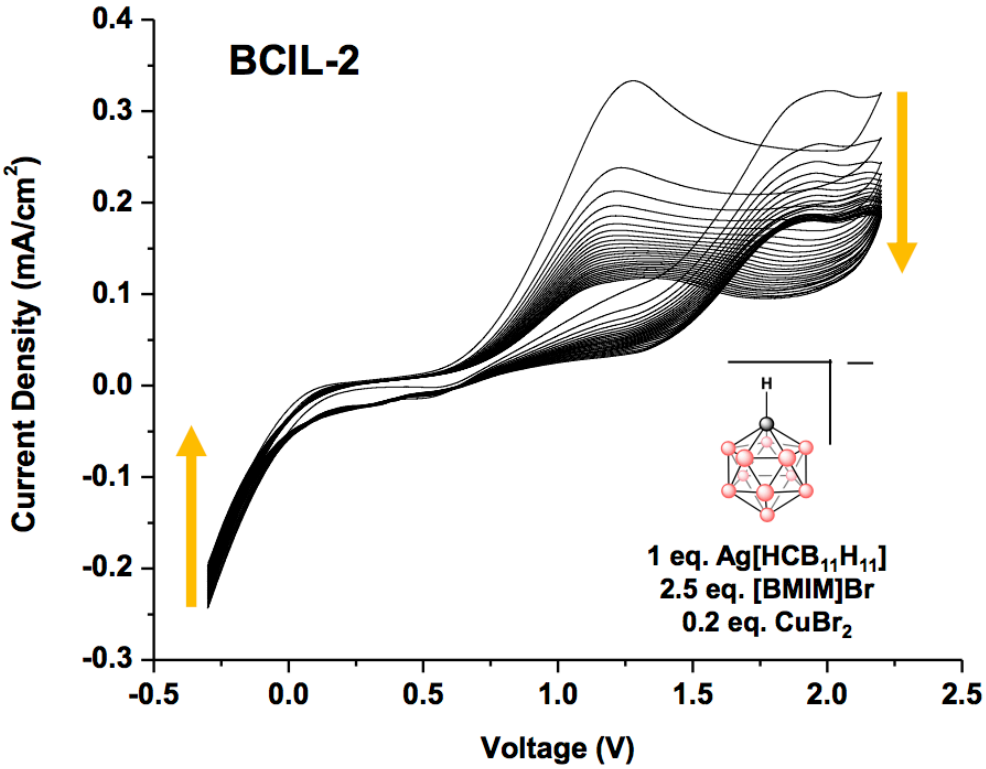

Figure S3. Decay of BCIL-2 current after 100 CV cycles.

ITO Degradation

A series of experiments on the reversible plating of Ag from BCIL-3 were conducted on both FTO and ITO slides. Significant reduction in device current was seen for ITO sandwiched BCIL-3 after only 100 cycles of current sweeping. Conversely, BCIL-3 sandwiched between FTO substrates displayed current consistency up to 2,000 cycles.

ITO degradation mechanism has been previously reported. Under the presence of an electric field, scratches at the ITO surface initiate degradation. Degradation is exacerbated by increased ITO surface area, the presence of external contaminants such as water and higher device operating temperatures.[4] Measurement of resistivity increase across ITO surface has also been attributed to surface growths, leading to degradation.[5] Such susceptibility to external factors presents manufacturing challenges if BCIL devices were to be implemented in spacecraft thermal control. FTO is a desirable alternative by introducing cycling stability without the need for strict monitoring of surface conditions.

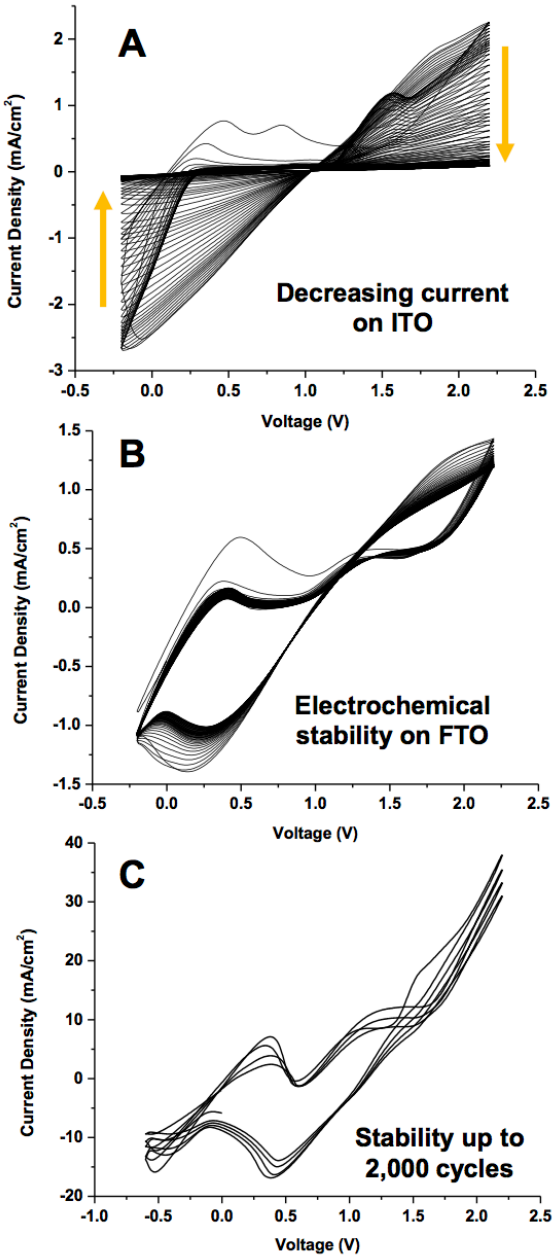

Figure S4. A) decreasing current of BCIL-3 on ITO after 100 CV cycles, B) stable electrochemical performance of BCIL-3 on FTO after 100 CV cycles, C) stable electrochemical performance of BCIL-3 on FTO after 2000 cycles.

Current Loss Upon Cooling to Room Temperature

As described in text, devices containing **BCIL2** and **BCIL3** were kept at room temperature overnight resulting in the decay of electrochemical features. To further display this "freeze-thaw" phenomenon a second figure detailing the before and after cooling state is attached herein.

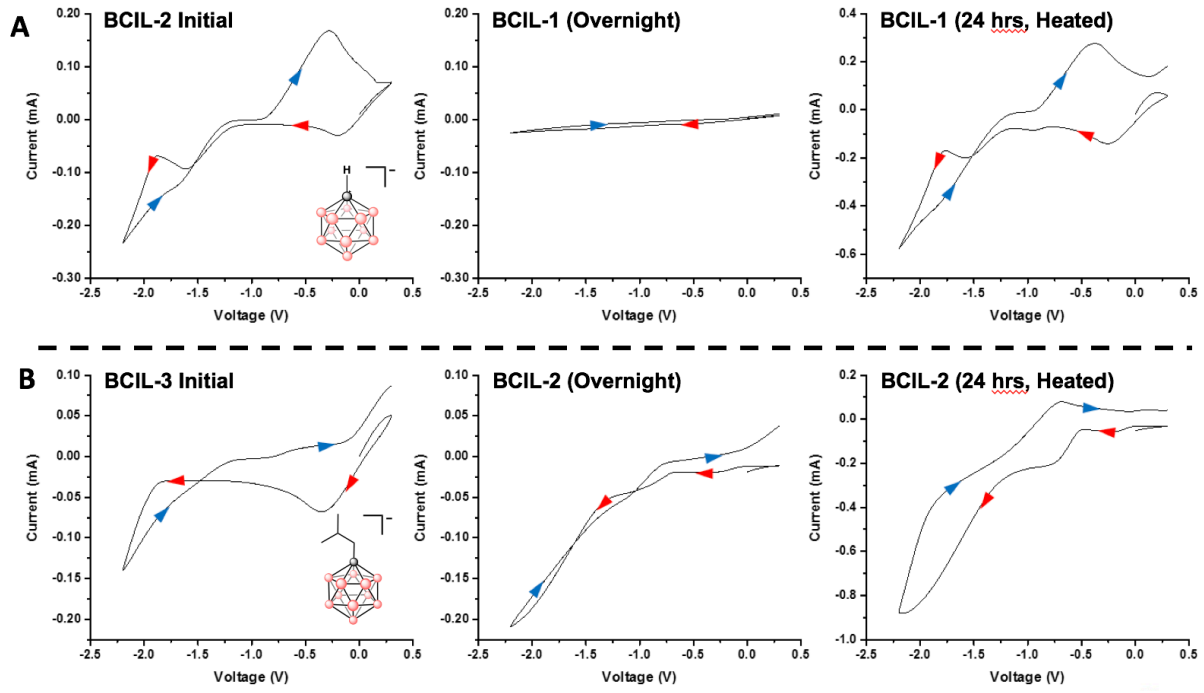

Figure S5. A) Two-electrode cyclic voltamograms of **BCIL-2** before and after equilibrating at ambient conditions overnight and after heating the equilibrated cell to 60 °C, top and bottom respectively. B) Two-electrode cyclic voltamograms of **BCIL-3** before and after equilibrating at ambient conditions overnight and after heating the equilibrated cell to 60 °C, top and bottom respectively.

8. Variable IR Emission

Silver Modulates Emissivity

A heated glass slide, coated on one side with a 100 nm thick silver film displayed drastically different emissivity depending on which side is facing the detector. When the uncoated glass side is facing the camera, the glass slide appears "hot", (Figure S5A). When the glass slide is flipped, the silver mirror is facing the detector and the substrate appears "cold", (Figure S5B). This apparent difference in temperature is due to the different emissivity of the top surface. Glass appears "hot" because it is an IR absorber (IR absorber at $\lambda<4$ μm), while silver films are IR reflective (<10% IR absorption).[6] Using this unique property, the thermal emissivity of a spacecraft could be controlled by deploying IR reflective surfaces (metallic films).

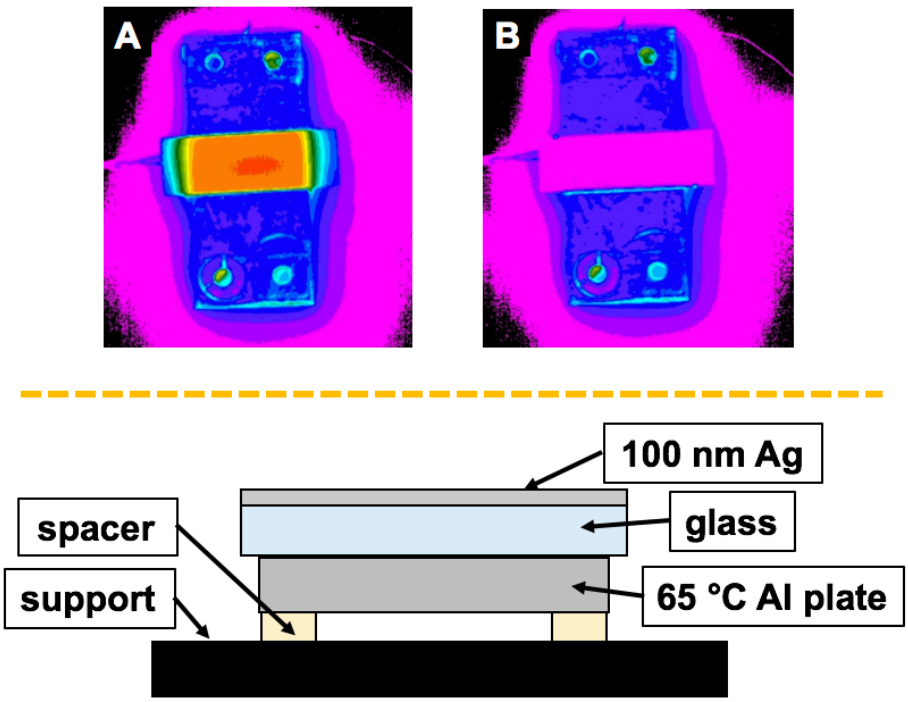

Figure S6. Top, A) strong IR emission observed when the glass side is facing up, B) strong IR reflection when the 100 nm silver film is facing up. Bottom, cross-section schematic of substrate emissivity experiment.

ITO-Sapphire IR Absorptive

Reported % change in transmittance value of 18% is believed to be largely affected by IR absorption of the sapphire substrate. Sapphire begins absorbing at ~2500 cm^{-1} (4 μm) and is not IR transparent beyond ~1700 cm^{-1} (5.8 μm), representing a majority of the IR range measured.[7] The limit to IR transmittance can be seen by thermal imaging of an ITO-coated sapphire electrode and a sapphire window on a heated silver surface, (Figure. S6). High heated intensity (blue) is seen for the sapphire window and even higher heat absorption is seen for ITO coated sapphire (green). Importantly, the IR reflectivity of the silver surface is masked by the IR absorptive (emissive) sapphire and ITO-coated sapphire windows. Although we were unable to achieve large changes in IR transmission and reflectivity, these experiments support the feasibility of a BCIL variable emissivity device. Further research efforts to improve BCIL device performance would focus on developing IR transparent electrodes suitable for thermal control applications.

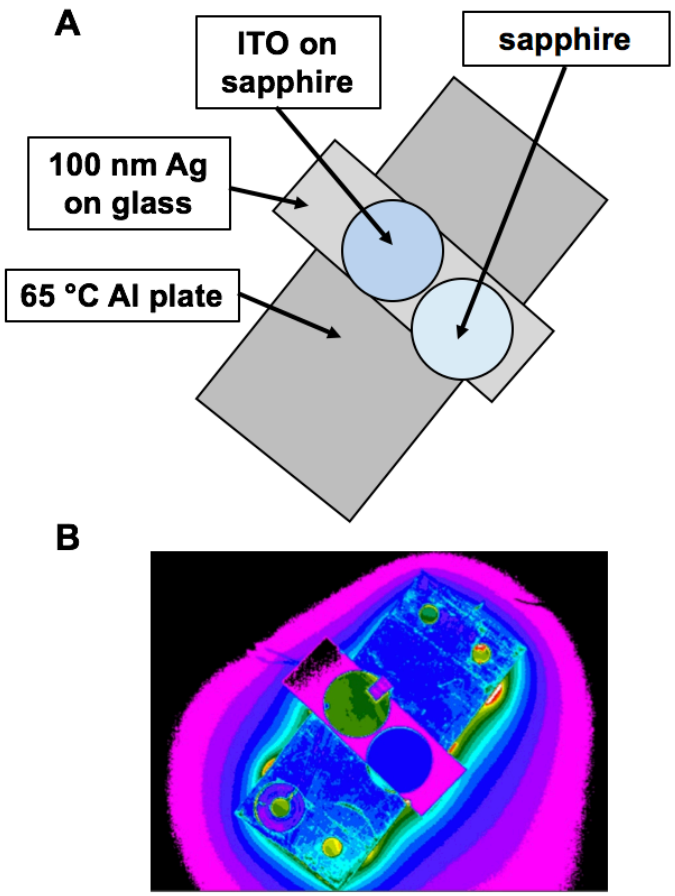

Figure S7. A) schematic of substrate emissivity experiment. B) near-IR thermal camera image of ITO coated and uncoated sapphire windows placed on an IR reflective (non-emissive) silver mirror on glass.

9. SEM Cross Section

In order to assess film thickness in the absence of acetonitrile washing, devices were disassembled and broken in half to image the cross section. An average film thickness of (244 ± 4) μm was determined. EDX measurements indicate excess carbon on towards the top of the film, likely residual ionic liquid. Silver is dispersed throughout, with pockets of higher concentration as consistent with a nucleation limited growth pattern.

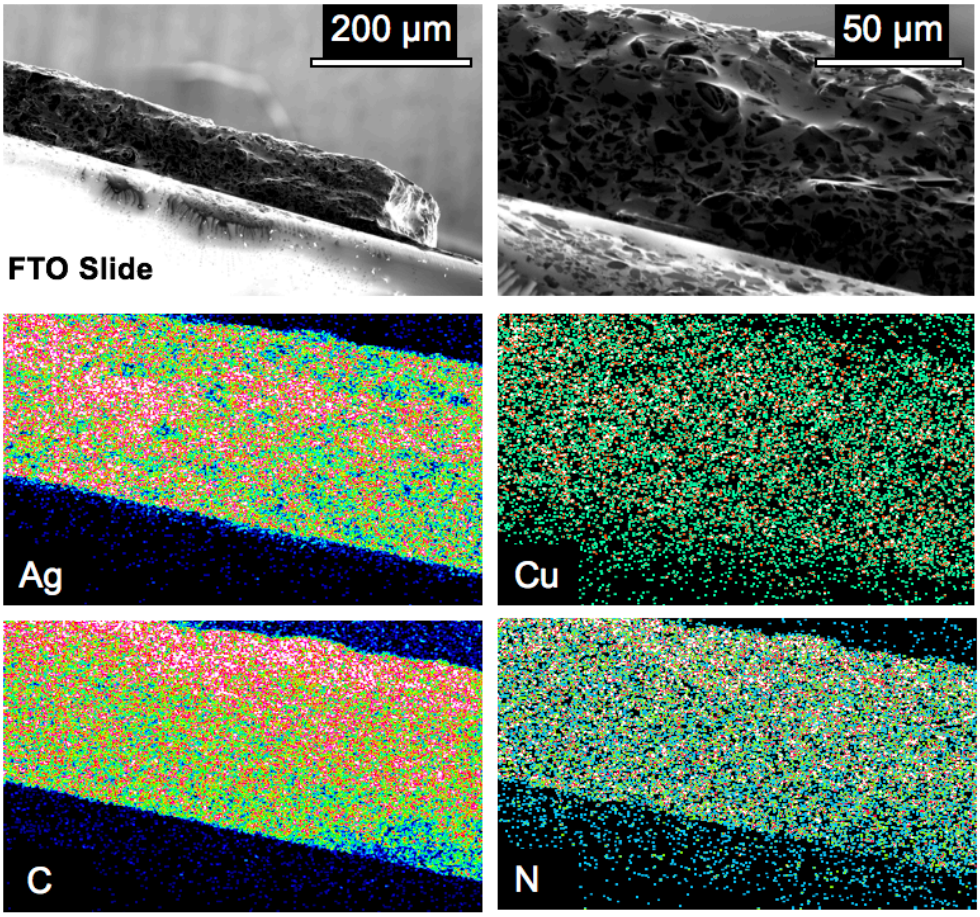

Figure S8. Cross-sectional scanning electron micrographs and EDX elemental mapping of BCIL-3 working electrode after deposition of a silver film. Average film thickness was calculated to be (244 ± 4) µm.

11. Video of Ag Plating and Dissolution

12. References

1) Shelly, K.; Finster, D.C.; Lee, Y.G.; Scheidt, W.R.; Reed, C.A. *J. Am. Chem. Soc*. **1985**, *107*, 5955.
2) Reed, C.A. *Acc. Chem. Res.*, **2010**, *43*, 121–128.
3) Jelinek, T.; Baldwin, P.; Scheidt, R.; Reed, C.A. *Inorg. Chem.* **1993**, *32*, 1982.
4) Leung, W.S.; Chan, Y.C.; Lui, S.M. *Mictroelectron. Eng*. **2013**, *1*, 1-7.
5) Park, G.; Kwon, J. *J. Mater. Sci.* **2001**, *12*, 497-503.
6) Clawson, J.F.; Tsuyuki, G.T.; Anderson, B.J.; Justus, C.G.; Batts, W.; Ferguson, D.; Gilmore, D.G. Spacecraft Thermal Environments. In *Spacecraft Thermal Control Handbook*; Ed.2; The Aerospace Press, 2002; vol. 1; 21-69.
7) Lowry, S. Analysis of Rubies and Sapphires by FT-IR Spectroscopy; *Thermo Fischer Scientific*; Madison, WI; Application Note 51124; 2008.